FERRIMAGNETIC ORDERING OF $Ca_2(Fe,Ni)MoO_6$ PEROVSKITES

E. BURZO[1], I. BALASZ-MURESAN[1]

[1]*Faculty of Physics, Babes-Bolyai University 40084 Cluj-Napoca, Romania, E-mail: emil.burzo@phys.ubbcluj.ro, Email: ibalasz@gmail.com*

Abstract. The $Ca_2Fe_{1-x}Ni_xMoO_6$ perovskites with $x \leq 0.2$ crystallize in a monoclinic $P2_1/n$-type structure. The lattice parameters increase parallelly with the nickel content. The perovskites are ferrimagnetically ordered, the saturation magnetization decreasing as result of nickel substitution. The reciprocal susceptibilities show non-linear temperature dependences. Assuming a two sublattices model, the distribution of ions, their valence states as well as the exchange interactions parameters between and inside magnetic sublattices were determined. These values are discussed in correlation with perovskite compositions.

Key words: Perovskites, crystal structures, magnetic properties.

1. INTRODUCTION

The aristotype cubic ordered double perovskites $A_2BB'O_6$ may be described as formed by corner sharing BO_6 and $B'O_6$ octahedra, alternating in all three directions. The A site cations occupy the cavities formed by the corner sharing octahedral network. Generally, the crystal structures of perovskites have lower symmetry than that above mentioned. Thus, the Ca_2FeMoO_6 perovskite crystallizes in a monoclinic type lattice having $P2_1/n$ space group [1]. The FeO_6 and MoO_6 octahedra are tilted due to the relatively small size of Ca^{2+} cation [2]. The ordering of Fe and Mo cations in B and B' sites, respectively is not perfect, the "antisite" defects being of $\cong 6$ % [3]

The neutron diffraction studies performed on Ca_2FeMoO_6 double perovskite evidenced an antiparallel alignment of Fe and Mo moments. Values $M_{Fe} = 4.0(1)$ μ_B and $M_{Mo} = 0.2(3)$ μ_B [4], $M_{Fe} = 3.2(1)$ μ_B and $M_{Mo} = 0.76(5)$ μ_B [2] or $M_{Fe} = 3.91(7)$ μ_B and $M_{Mo} = 0.7(3)$ μ_B [5] were reported. The saturation magnetization, according to different authors, ranges from $\cong 3.50$ to 3.60 μ_B/f.u. [1, 3-8] and the Curie temperature has been located between $T_c = 345$ K [1] and 380 K [2, 6]. An excess of iron ions contributed significantly to the increase of T_c values [9].

Above the magnetic ordering temperature, the reciprocal susceptibility, χ^{-1}, was considered to follow a Curie-Weiss type behaviour [3, 6]. The reported Curie constant, C and paramagnetic Curie temperature, θ_p, were C = 2.10 Kemu/mol, θ_p = 420 K [3] or C = 3.64 Kemu/mol and, θ_p = 398 K [6], respectively. A non-linear temperature dependence of χ values in Ca_2FeMoO_6 perovskite was also shown [8].

In this paper we analyse the magnetic properties of $Ca_2Fe_{1-x}Ni_xMoO_6$ perovskites with $x \leq 0.2$, in a large temperature range. The locations of transition

metal ions, in B and B' sites, as well as their valence states, are analysed in correlation with samples compositions.

2. EXPERIMENTAL

The $Ca_2Fe_{1-x}Ni_xMoO_6$ perovskites with $x \leq 0.2$ were prepared by solid state reaction. The stoichiometric quantities of $CaCO_3$, Fe_2O_3, NiO and MoO_3 powders were mixed and calcinated in argon atmosphere at T = 900 ^oC. The calcinated powders were peletized and sintered at 1300 ^oC, during 8 hrs, in argon atmosphere having 3 % hydrogen. The sintering time has been shown to be an important parameter in obtaining good quality samples [10].

The phase purity, crystal structures and lattice parameters have been determined by X-ray diffraction, by using a Seifert-type equipment. The X-ray patterns were analysed by Rietveld method by using a TOPAS program [11].

Scanning electron microscopy (SEM) and energy dispersive spectroscopy (EDS) measurements were made by using a JEOL-type equipment on polished samples. The grain sizes, as well as and the distribution of constituting elements inside the grains, were analysed.

Magnetic measurements were performed by extraction method in the temperature range 4 K $\leq$ T $\leq$ 780 K and fields up to 120 kOe. Above T_c, the magnetic susceptibilities, χ, were determined according to Honda-Arrott plots, from their field dependences, $\chi_m = \chi + cM_iH^{-1}$, by extrapolating the measured values at $H^{-1} \rightarrow 0$ [12]. By c is denoted a possible magnetic ordered impurity content having M_i saturation magnetization. When using this method, any possible alteration of χ values is avoided, if the measurements are performed in external fields higher than the saturation one.

3. RESULTS

3.1 Crystal structures

The room temperature XRD patterns of $Ca_2Fe_{1-x}Ni_xMoO_6$ perovskites indicated the presence of a single phase double perovskite, in the composition range $x \leq 0.2$, as exemplified in Fig.1 for samples with x = 0 and 0.2. These crystallize in a monoclinic type structure having space group $P2_1/n$. The lattice parameters increase as the nickel content is higher – Fig.2. This behaviour can be correlated with greater Ni^{2+} ionic radius (0.69 Å) as compared to those of Fe^{3+} (0.645 Å) or Fe^{2+} (0.61 Å) ions situated in 6–coordination. There is a linear composition dependence of the cell volumes – Table 1. The monoclinic angles are close to 90^o, indicating a strong pseudo-orthorhombic character of the unit cell. The distortions of CaO_{12} polyhedra decrease from $4.9 \cdot 10^{-2}$ (x = 0) to $2.87 \cdot 10^{-2}$ (x = 0.2) as the nickel content increases.

Table 1
Samples compositions and magnetic properties

x	Composition	Mean grain size(Å)	Volume (Å^3)	M_S (μ_B/f.u.)	T_c (K)	
					exp.	calc.
0	$Ca_2Fe_{1.02}Mo_{0.955}O_{5.92}$	23.5	230.379	3.49	367	362
0.1	$Ca_2Fe_{0.922}Ni_{0.09}Mo_{1.02}O_{6.10}$	25.0	231.209	3.43	330	336
0.2	$Ca_2Fe_{0.81}Ni_{0.185}Mo_{0.99}O_{6.06}$	24.0	232.428	3.36	323	326

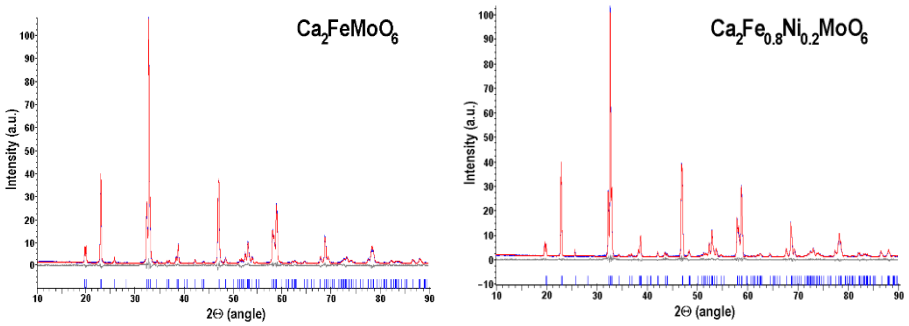

Figure 1 - XRD patterns of $Ca_2Fe_{1-x}Ni_xMoO_6$ perovskites with x = 0 and 0.2.

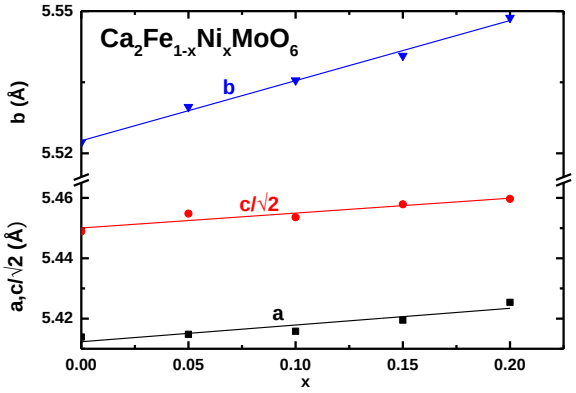

Figure 2 - Composition dependences of the lattice parameters.

The antisite (AS) content has been determined – Fig.3. From the ratio, r of I(101)/{I(200)+I(112)} line intensities, values between 5.8 % (x = 0) to 9.4 % (x = 0.2) were obtained. A somewhat higher AS content, for samples with $x \leq 0.05$, has been estimated from refinement of XRD patterns. For higher nickel content, these are close to those determined from r ratio. When starting from charge neutrality condition and magnetic data, the antisite content was shown to be rather close to those obtained from line intensities ratio.

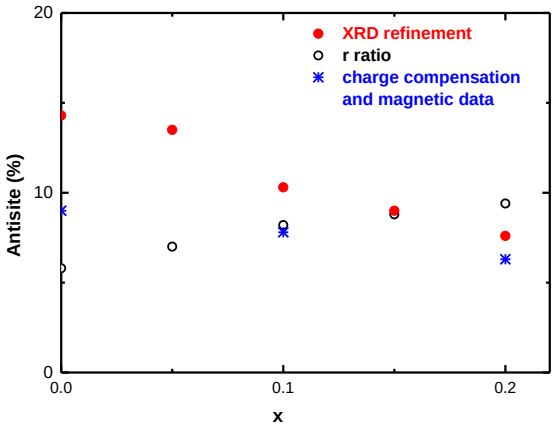

Figure 3 - The antisite content determined from I(101)/{I(200)+I(112)} line intensity ratio (○), XRD refinement (●) and charge neutrality condition and magnetic data (★).

The samples compositions and grain dimensions were determined by SEM and EDS measurements. The grain dimensions are situated in the range 20 – 70 Å, somewhat higher than the mean values determined from the Scherrer equation (≅ 25 Å). The samples compositions are little different from those of starting mixtures – Table 1.

The variable valences components of the $Ca_2Fe_{1-x}Ni_xMoO_6$ perovskites, can be described by the $Fe_u^{3+}Fe_{1-u}^{2+}Mo_v^{5+}Mo_{1-v}^{6+}$ normalized formula. Starting from the determined compositions, according to charge neutrality rule, the relations between u and v parameters were determined [10]:

$$u\text{-}v = 0.1\ (x = 0),\ 0.056\ (x = 0.1),\ 0.17\ (x = 0.2) \qquad (1)$$

These data will be further considered in order to analyse the valence states of transition metal ions in the above perovskites

3.2 Magnetic properties

The temperature dependences of the magnetizations in zero field cooled (ZFC) and 1 kOe field cooled (FC) samples, having nominal nickel content x = 0, 0.1 and 0.2 are given in Fig. 4. There are relative small irreversibilities, at temperatures T < 280 K, evidencing the presence of a cluster glass contribution to the magnetizations. The saturation has been obtained in external fields higher than H = 20 kOe – Fig.5. These data suggest that the clusters magnetizations are aligned in the external fields higher than the above value.

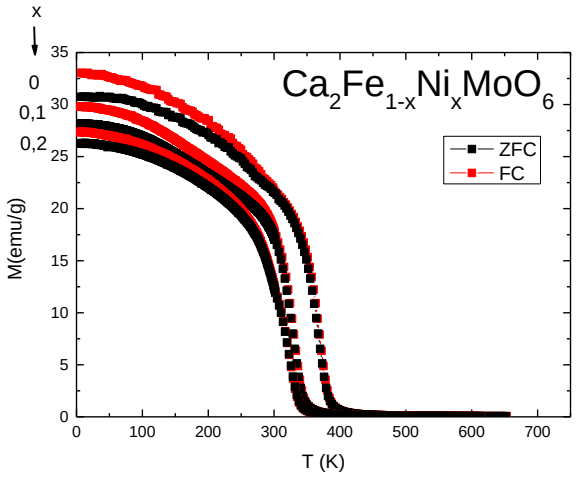

Figure 4 - Temperature dependences of the magnetizations in zero field cooled (ZFC) and 1 kOe field cooled (FC) perovskites.

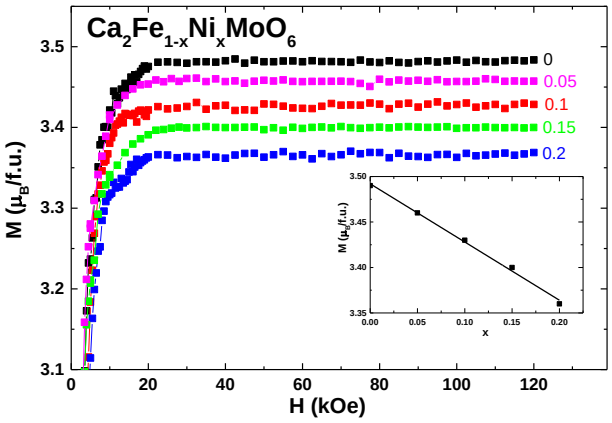

Figure 5 - Magnetization isotherms, at 4 K. In inset is plotted the composition dependence of the saturation magnetizations.

The studied perovskites are ferrimagnetically ordered. The saturation magnetizations, at 4 K, decrease nearly linearly when increasing the nickel content, with a slope of s ≅ 0.7 μ_B per substituted nickel atom. The s slope is by three times smaller than expected if Ni^{2+} ions replace the ferrous ones at the B site, suggesting a more complex process including also changes in the valence states of some ions.

In analysing the magnetic data, ordered moments of 5 μ_B, 4μ_B and 2μ_B are assumed for ferric, ferrous and nickel ions. As already mentioned, there is a large discrepancy between the molybdenum magnetic moment, determined by neutron diffraction in Ca_2FeMoO_6 [2, 4, 5]. This originates from the fitting procedure

which do not allowed determination of M_{Mo} with a good accuracy. A reliable value for the molybdenum moment was obtained by X-ray magnetic circular dichroism on Sr_2FeMoO_6 single crystal [13]. As already discussed [14], we use the value of 0.32 μ_B, for describing the molybdenum ordered moment also in the present system.

The thermal variations of reciprocal susceptibilities show non-linear behaviour, characteristic for ferrimagnetic systems – Fig.6. A two sublattices model, corresponding to B and B' sites was assumed in order to analyse the magnetic data. In this model, the temperature dependences of the magnetic susceptibilities can be described by the Néel type relation [15]:

$$\frac{1}{\chi}=\frac{1}{\chi_0}+\frac{T}{C}-\frac{\sigma}{T-\theta} \qquad (2)$$

By C is denoted the Curie constant and $1/\chi_0$, σ and θ are parameters related to the exchange interactions inside and between the magnetic sublattices.

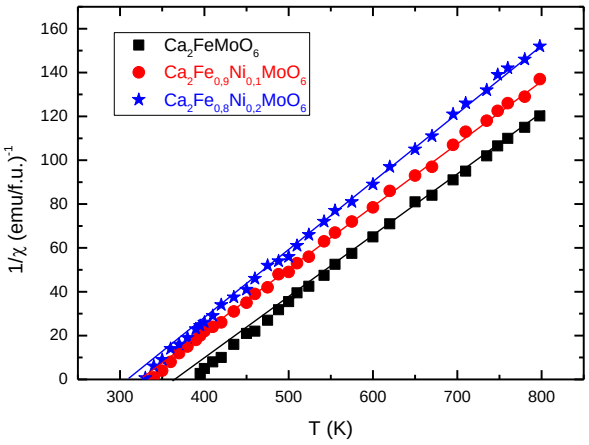

Figure 6 - Thermal variations of reciprocal susceptibilities for $Ca_2Fe_{1-x}Ni_xMoO_6$ perovskites with x = 0, 0.1 and 0.2.

The deviations of χ^{-1} vs T from a linear dependence, as evidenced at relative lower temperatures ($T_c < T < 500$ K), are rather small. This seems to be the reason why the already reported data on Ca_2FeMoO_6 were assumed to follow a Curie-Weiss type behaviour [5, 6].

The Curie constants, C, determined in the asymptotic temperature range (T> 400 – 450 K), decrease as the nickel content is higher. Admitting an ionic model, where the Curie constants of constituting elements are given by their free ion values, according to addition law of magnetic susceptibilities we have:

$$C=uC_{Fe^{3+}}+(1-u)C_{Fe^{2+}}+vC_{Mo^{5+}} \qquad (3)$$

Starting from the relations (1) and (3), the distributions of constituting ions in B and B' sites were determined and compared with those obtained from XRD refinements – Fig.7. Although the same trend is evidenced, the fractions of iron and molybdenum ions at B sites are somewhat higher than those determined from

structural studies. The differences can be correlated with a higher AS content estimated in the last case.

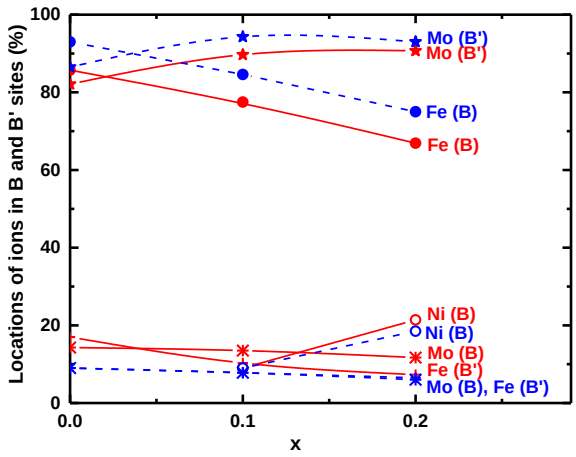

Figure 7 - The locations in B and B' sites of iron, nickel and molybdenum ions as determined from XRD refinements (blue points) and charge neutrality condition and Curie constants (red points), respectively.

The valence states of ions located in B and B' sites were determined in order to fit the composition dependence of the saturation magnetizations. The Fe^{3+} and Mo^{5+} ions have been located in antisites at B' and B positions, respectively – Fig.8. The AS fraction increased beyond that estimated from structural studies if the B' antisite will be populated by ferrous ions.

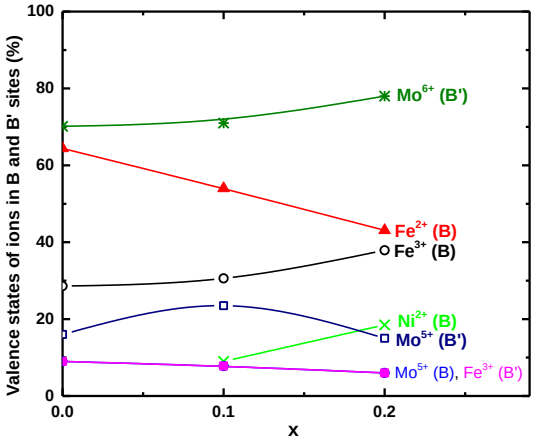

Figure 8 - The fractions and valence states of the ions located at B and B' sites.

The exchange parameters characterizing the interactions inside (α, β) as well as between magnetic sublattices (n), were determined by using the mean field model [15] – Table 2. The n values are negative as expected in case of ferrimagnetic type ordering. These values decrease in absolute magnitude as result

of nickel substitutions. The reliability of the above data was confirmed by computing the Curie temperatures taking into account the determined exchange interaction parameters. The T_c ones, thus obtained, are only by 1-2 % different from experimental values, as evidenced in Table 1.

Table 2

Data obtained from paramagnetic measurements

x	χ_0^{-1} (emu/f.u.)$^{-1}$	C (Kemu/f.u.)	σ (emu/f.u.)$^{-1}$K	θ (K)	Exchange interactions parameters		
					α	β	-n
0	-96.4	3.67	520	331	6.2	35.8	18.7
0.1	-91.3	3.51	112	322	7.7	51.3	14
0.2	-97	3.21	84	311	8.0	69.2	13.8

4. CONCLUSIONS

The $Ca_2Fe_{1-x}Ni_xMoO_6$ double perovskites having compositions $x \leq 0.2$, crystallize in a monoclinic type structure having $P2_1/n$ space group. The lattice parameters increase parallelly with nickel content.

The perovskites are ferrimagnetically ordered, the magnetic moments at B and B' sites being antiparallelly oriented. The decrease of the saturation magnetizations, as effect of Ni substitution, can be correlated mainly with their location at B sites where these replace the ferrous ions.

Starting from the charge neutrality condition and magnetic data, the locations and valence states of constituting ions were obtained. The antisite content, determined both from XRD and magnetic data, are of the order of 8 %.

The reciprocal susceptibilities follow non-linear temperature dependences of Néel-type, characteristic for ferrimagnetic type ordering. When increasing nickel content, the χ^{-1} vs T curves approaches to linear dependences. These can be correlated with the relative magnetic contributions of the two sublattices. Those at B' site decrease, in the studied compositions range, from 13.2 % (x = 0) to 10.5 % (x = 0.2), the dominant ones in describing the magnetic properties, being those of the B sublattices. The exchange interactions inside and between magnetic sublattices were determined assuming a two-sublattice model. The interaction parameters between the B and B' sublattices are negative and decrease in absolute magnitude as the nickel content is higher. By using the exchange interactions constants, experimentally determined, the Curie temperatures are correctly described.

REFERENCES

[1] R.P.Borges, R.M.Thomas, C.Cullinan, J.M.D.Coey, S.Suryanarayanan, L. Ben-Dor, I.Pinsard-Gaudart, A, Revcolevski, J. Phys.: Condens. Matter **11**, L445 (1999).

[2] J.A.Alonso, M.T.Casais, M.J.Martinez-Lope, J.L.Martinez, P.Velasco, A.Munoz, M.T.Fernandez-Diaz, Chem. Mater. **12**, 161 (2000).

[3] D.Rubi, J. Nogues, J.S.Munoz, J.Fountcuberta, Mat. Sci. Eng. **B126**, 279 (2006).
[4] I.Pinsard-Goudart, R.Surynarayanan, A.Revcolevschi, J.Rodriguez-Carvajal, J.M.Greneche, P.A.J.Smith, R.M.Thomas, R.P.Borges, J.M.D.Coey, J. Appl. Phys. **87**, 7118 (2000).
[5] C.Ritter, M.R.Ibarra, L.Morellon, J.Blasco, J.Garcia, J.M.De Teresa, J. Phys.: Condens. Matter **12**, 8295 (2000).
[6] N.O.Moreno, L.B.Barbosa, D.R.Ardila, J.P.Andreeta, J. Super. Novel Magn. **26**, 2501 (2013).
[7] Y.Yasukawa, J.Linden, T.S.Chan, R.S.Liu, H.Yamauchi, H.Karppinen, J. Solid State Chem. **177**, 2655 (2004).
[8] E.Burzo, I.Balasz, AIP Conf. Proc. **1722**, 080003 (2016).
[9] D.Rubi, C.Frontera, A.Roig, J.Nogues,J.S.Munoz, J.Fontcuberta, J.Phys.: Condens. Matter **17**, 8037 (2005).
[10] E.Burzo, I.Balasz, M.Valeanu, D.P.Kozlenko, S.E.Kichanov, A.V.Ratkauskas, B.N.Savenko, J. Alloys Comp. **621**, 71 (2015).
[11] DIFRAC plus TOPAS General Profile and Structural Analysis Software for Powder Diffraction Data, USERS's MANUAL, Version 20, Bruker 20, Bruker AXS Gmb Karlsruhe, 2001.
[12] L.M.Bates, Modern Magnetism, Cambridge University Press, 1951, p. 139.
[13] M.Besse, V.Cros, A.Barthelemy, H. Jaffres, J. Vogel, F.Petroff, A.Mirone, A.Tagliaferi, P.Bencok, P. Decorse, P. Berthet, Z.Szotek, W.M.Temmerman, S.S.Dhesi, N.B.Brookes, A.Rogalev, A.Fert, Europhys. Lett. **60**, 608 (2002).
[14] E.Burzo, D.P.Kozlenko, N.T.Dang, S.E.Kichanov, N.O.Golosova, J. Alloys Comp. **664**, 363 (2016)
[15] L. Néel, J. Phys. (Paris) **3**, 137 (1948).